

Development of a coupled thermo-hydro-mechanical double structure model for expansive soils

David Mašín¹

¹Faculty of Science, Charles University in Prague, Czech Republic

Abstract. In this paper, development of a thermo-hydro-mechanical model for expansive soils including double structure is described. The model is based on hypoplastic model by Mašín [6], in which the hydro-mechanical coupling is considered at each of the two structural levels. The model also includes separate effective stress definitions and water retention curves for the two levels of structure. In the proposed model, an approach by Mašín and Khalili [8] to include thermal effects into hypoplastic models is followed. This is combined with temperature-dependent water retention curve of macrostructure, temperature-induced deformation of microstructure and an enhanced double-structure coupling law. Good predictions of the model are demonstrated by comparing the model simulations with experimental data on MX80 bentonites taken over from literature.

1 Introduction

Thermo-hydro-mechanical modelling of the behaviour of expansive clays is important in a number of high-priority applications, such as design of nuclear waste repositories. Their behaviour is, however, remarkably complex, in particular due to their double-structure nature. Each of the structural levels respond differently to temperature change, suction change and mechanical action. In this paper, an advanced model is developed aiming to predict these complex phenomena in a unified manner.

2 Double structure model

The model described in this paper has been developed using double-structure framework, originally proposed by Alonso et al. [1]. The model is based on the hydro-mechanical double structure hypoplastic model by Mašín [6]. This model is briefly described in Sec. 2.1.

2.1 Existing hydro-mechanical model

The double structure models are based on the assumption supported by various micro-mechanical studies that in expansive soils one can identify two levels of structure: So-called macrostructure, which is representing an assembly of silt-size aggregates of the clay particles, and so-called microstructure, which is representing the internal structure of these aggregates. A conceptual sketch of these two levels of structure is in Fig. 1.

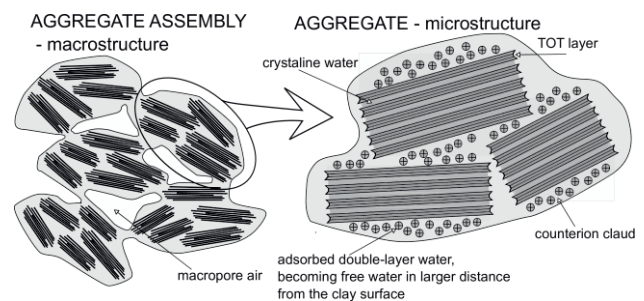


Figure 1. A conceptual sketch of two levels of structure considered in double-structure models (from [6]).

In the model by Mašín [6], separate models are considered for mechanical and hydraulic responses of microstructure and macrostructure. These responses are coupled at the given structural level, and additionally, the behaviour of the two structural levels is linked through the double-structure coupling function.

Mašín [6] based the mechanical model for the behaviour of macrostructure on the model by Mašín and Khalili [7]. Hydraulic response of macrostructure was based on the void-ratio dependent water retention model [4]. Microstructure has always been considered as fully saturated and its behaviour was governed by the Terzaghi effective stress principle: see Mašín and Khalili [9] for thorough discussion of this subject. The double structure coupling is controlled by a function of relative void ratio, which evolved from the original proposition by Alonso et al. [1].

^a Corresponding author: masin@natur.cuni.cz

2.2 Proposed thermo-hydro-mechanical model

In the proposed model, thermal effects on the behaviour of macrostructure and microstructure have been incorporated. The model [6] has been enhanced in the following way:

- A new mechanical hypoplastic model for saturated soils (Mašin [5]) is adopted as a base mechanical model for macrostructure.
- The thermal behaviour of macrostructure is described by an approach developed by Mašin and Khalili [8]. The model assumes temperature-dependent normal compression lines of the form

$$\ln(1 + e) = N(s, T) - \lambda^*(s, T) \ln\left(\frac{p^M}{p_r}\right) \quad (1)$$

where p^M is the effective mean stress of macrostructure, p_r is the reference stress of 1 kPa, s is suction and T is temperature (measured in Kelvins). $N(s, T)$ and $\lambda^*(s, T)$ are temperature- and suction-dependent positions and slopes of normal compression lines, respectively. They are defined as

$$N(s, T) = N + n_s \left\langle \ln \frac{s}{s_e} \right\rangle + n_T \ln \frac{T}{T_r} \quad (2)$$

$$\lambda^*(s, T) = \lambda^* + l_s \left\langle \ln \frac{s}{s_e} \right\rangle + l_T \ln \frac{T}{T_r} \quad (3)$$

where N , n_s , n_b , l_s , l_t are parameters and T_r is a reference temperature.

- The water retention model for macrostructure is based on the hysteretic model from [6], where the air-entry value of suction $s_{en}(T)$ is considered to be temperature-dependent. It is controlled by an equation

$$s_{en}(T) = s_{en} \left(\frac{a+bT}{a+bT_r} \right) \quad (4)$$

s_{en} the air-entry value of suction for macrostructure, which is void ratio dependent and it is calculated using approach from [4]. This model requires two parameters, namely reference air-entry value of suction s_{en0} for the reference macrostructural void ratio e_0^M . a and b in Eq. (4) are parameters. As pointed out by Grant and Salehzadeh [2], their values $a=0.18$ N/m and $b=-0.00015$ N/(mK) imply that the effects of temperature by water retention capacity are caused solely on its effect on surface tension. This has not been supported by experimental observation, however (Romero et al. [3]).

- Microstructure is considered to be fully saturated. Following the work by Mašin and Khalili [9], its mechanical response is considered to be governed by the Terzaghi effective stress principle with additional strains induced by temperature variation. The thermal deformation is considered to be fully reversible, governed by the coefficient α_s , using

$$\dot{\epsilon}^{mT} = \frac{1}{3} \alpha_s \dot{T} \quad (5)$$

where $\dot{\epsilon}^{mT}$ are thermal strains of microstructure and $\mathbf{1}$ is the second-order identity tensor.

- Integration of Eq. (5), together with the equation controlling volumetric response of microstructure due to the change of microstructural effective stress, can be used for initialisation of the microstructural void ratio e_m . The equation reads:

$$e^m = \exp \left[\kappa_m \ln \left(\frac{s_r}{p^m} \right) + \ln(1 + e_{r0}^m) + \alpha_s (T - T_r) \right] - 1 \quad (6)$$

where p^m is the microstructural effective mean stress and e_{r0}^m , κ_m and s_r are parameters.

- In the original model, the double structure coupling function f_m has been assumed as zero for aggregate shrinkage. In the present model, however, this assumption leads to underprediction of global shrinkage in cooling experiments. The experimental data (Fig. 4) indicate that the global shrinkage in cooling depends on suction. The following equation has been proposed for particle shrinkage which was found to leads to good representation of experimental data:

$$f_m = c_{sh} \left(\frac{s}{s_e} \right) \quad (7)$$

where c_{sh} is a parameter. f_m is bound within the range 0 to 1.

The complete model takes the following rate form:

$$\dot{\sigma}^M = f_s [\mathcal{L} : (\dot{\epsilon} - f_m \dot{\epsilon}^m) + f_d \mathbf{N} \|\dot{\epsilon} - f_m \dot{\epsilon}^m\|] + f_u (\mathbf{H}_s + \mathbf{H}_T) \quad (8)$$

where \mathcal{L} , \mathbf{N} , \mathbf{H}_s and \mathbf{H}_T are hypoplastic tensors, f_s , f_d and f_u are hypoplastic scalar factors, $\dot{\epsilon}$ is the Euler stretching tensor, $\dot{\sigma}^M$ is the objective effective stress rate of macrostructure and $\dot{\epsilon}^m$ is microstructural strain rate. Due to the space restrictions, it is not possible to describe Eq. (6) in detail, the interested readers can refer to [6, 7, 8] for thorough explanation of the model components.

It is to be pointed out that for the general case of a test with controlled stretching, suction rate and temperature rate, and unknown rates of total stress and degree of saturation, solution of Eq. (6) is not straightforward: total stress rate appears both in the formulation of $\dot{\epsilon}^m$ and in the formulation of $\dot{\sigma}^M$, thus on both the right- and left-hand side of Eq. (6). A numerical procedure has been developed to solve this equation, and it has been implemented into an in-house general purpose thermo-hydro-mechanical single element code. This implementation has been adopted in the evaluation of the model presented in Section 3.

2.3 Model parameters

In this section, physical meaning of model parameters which have not been mentioned in Sec. 2.2 is briefly described. These parameters are identical to the parameters of the basic hydro-mechanical model [6] and the readers are referred to the original publication for more details.

- The basic model requires, additionally to the parameters from Sec. 2.2, to specify parameters φ_c (critical state friction angle in a standard soil-

mechanics meaning), ν (parameter controlling stiffness in shear) and κ^* (controls macrostructural volume strain in unloading).

- The parameter m is present at two places within the model formulation. First of all, it controls the factor f_u and thus the dependency of the wetting- and heating-induced compaction on the distance from the state boundary surface (the higher the value of m , the closer the state needs to be to the state boundary surface for the compaction to become significant). Second, the parameter m controls the double-structure coupling function and it thus affects the response to wetting-drying and heating-cooling cycles (see [6]).
- a_e is the ratio of air-entry and air-expulsion values of suction of the water retention model for macrostructure.

3 Model evaluation

3.1 Description of the material and experiments

The model has been evaluated with respect to experimental data on compacted bentonite by Tang and Cui [10] and Tang et al. [11]. They studied the behaviour of MX80 bentonite from Wyoming, USA, under non-isothermal conditions. Two experimental data sets have been adopted.

The first one has been published by Tang and Cui [10]. They studied water retention behaviour of a compacted bentonite in suction- and temperature-controlled isotropic cell. Prior to the test, the samples had the initial suction slightly lower than 145 MPa (140 MPa was assumed in the simulations) and the initial dry density was 16.5 kN/m^3 . Subsequently, different values of total suction were applied using vapour equilibrium technique and water content of samples was measured until it has stabilised.

The second experimental data set has been published by Tang et al. [11]. The samples have been tested in suction- and temperature-controlled isotropic cell capable of application of high suctions using vapour equilibrium technique, high temperatures (up to 80°C reached in the experiments from [11]) and high mechanical isotropic stresses (up to 60 MPa applied in [11]). Prior to the testing, compacted specimens with an initial suction of 110 MPa and dry densities of approx. 17.5 kN/m^3 were machined to obtain the required dimensions (80 mm in diameter, 10-15 mm in height). Thereafter, suction was changed using vapour equilibrium technique to the desired values (9, 39 and 110 MPa in three experimental sets) while measuring the swelling deformation. Samples were then placed into the cell and loaded to the initial isotropic total stress of 0.1 MPa. This was the initial state for subsequent thermo-mechanical testing. For the detailed description of the tests the reader is referred to [11].

3.2 Description of the modelling procedure

In the simulations, complete thermo-hydro-mechanical histories of the samples have been followed. That is, the initial state for the given thermo-hydro-mechanical

experimental stage has not been prescribed, but it has instead been simulated from the common initial state. All the water retention curve simulations were performed from the initial state of total suction $s_r=140 \text{ MPa}$, $e=0.64$, $T=25^\circ\text{C}$, $a_{scan}=1$ and zero total stress. The initial stage has been followed by a change of temperature to the desired value and subsequent suction variation under zero total stress. The initial void ratio was calculated from the initial dry densities using specific gravity of grains $G_s=2.76$, which was implied by the data in [11].

The samples tested in the suction- and temperature-controlled isotropic cell had all have the initial state of $s=110 \text{ MPa}$, $e=0.53$, $T=25^\circ\text{C}$, $a_{scan}=0$ and zero total stress. The initial stage has been followed by an (eventual) change of suction, increase of total stress to 0.1 MPa and increase of temperature. Subsequent testing followed the desired thermo-mechanical path.

3.3 Calibration of the model

Due to the limited number of available experiments, the model has been calibrated using the data to be predicted. Also, the experimental programme did not allow to calibrate all the model parameters. The additional parameters have been assumed using the previous experience. It is to be pointed out that the assumed parameters do not affect substantially the model predictions.

Parameters of the basic hypoplastic model λ^* and κ^* have been calibrated using isotropic compression experiments (Fig. 5). Parameters N , n_s , n_b , l_s , l_t and m were adjusted so the model properly predicted position of isotropic normal compression lines (Fig. 5) and also the heating-induced collapse/swelling strains (Fig. 4). Parameters φ_c and ν have been assumed.

Reference values s_r , e_0^M and T_r have been selected so they were within the range relevant for the present simulations. The corresponding e_{r0}^M has been adjusted for water retention curve predictions. The parameter κ_m controls both the swelling due to suction decrease (thermo-mechanical tests, Fig. 3) and water retention curves (Fig. 2). The value of κ_m has thus been selected to predict accurately the swelling tests, while it was observed that this value leads to overprediction of water content in water retention experiments. Note that as very large strains (up to 50%) were reached in swelling tests, the experimental data from [11] have been replotted in terms of natural strain for consistency with the modelling output.

The value of α_s is controlling the thermal-induced swelling, it has been calibrated using heating tests at the suction of 110 MPa (Fig. 4). The parameters controlling water retention curve of macrostructure have little influence on results at very high suctions, s_{e0} and a_e have thus been assumed and a and b have selected considering that the effects of temperature on water retention capacity are caused solely by its effect on surface tension.

The set of parameters adopted in all the simulations is given in Table 1.

Table 1. Parameters of the model adopted in all the simulations.

φ_c	λ^*	κ^*	N	ν	n_s	l_s
25	0.081	0.01	1.46	0.25	0.01	0.0045
n_t	l_t	m	α_s	κ_m	e_{r0}^m	c_{sh}
-0.07	0	10	0.00015 K ⁻¹	0.2	0.1	0.002
s_{e0}	a	b	a_e	s_r	e_0^M	T_r
200 kPa	0.118	-0.000154	0.75	140 MPa	0.5	294 K

3.4 Model predictions

Model predictions are shown in Figures 2 to 5.

The predicted water retention curves are in Fig. 2. It is clear that, although the model predicts correctly the swelling due to wetting (Fig. 3), it is overpredicting water content at lower values of suction (Fig. 2). These two facts are contradictory, and they can be caused by the fact that the two experimental data sets originate from different experimental data sets (albeit from the same soil mechanics laboratory). The samples also had different initial conditions, there can thus be slight variations in the soil structure, which affects soil properties.

As the model predicts aggregate swelling with heating, it also predicts slightly higher retention capacity of heated soil: the experiments appear to show the contrary, but the difference is small.

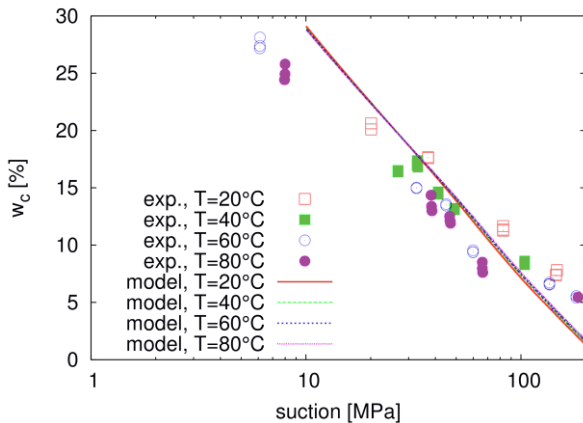


Figure 2. Water retention curves at different temperatures: experimental data [10] compared with model predictions.

Figure 3 shows swelling due to wetting at zero total stress and constant temperature 25°C as measured on samples which have later been placed into the suction- and temperature-controlled isotropic cell. Swelling is slightly underpredicted, which is a consequence of optimization of the model calibration so that also water retention curves are predicted reasonably. Recall that complete thermo-hydro-mechanical histories of the samples have been simulated, the state reached after the wetting stage thus represents the initial state for subsequent simulations.

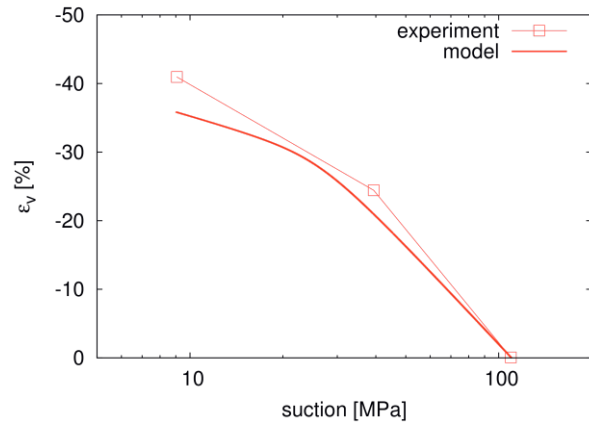


Figure 3. Swelling strains developed during wetting of the samples later tested in suction- and temperature-controlled isotropic cell. Experimental data [11] compared with model predictions.

Volume strains due to heating at various values of suction and mean total stress are shown in Figure 4. The model is accurately predicting the observed complex behaviour. In particular:

- At high suctions (110 MPa), the model is correctly predicting swelling, whose magnitude is controlled by the parameter α_s . The heating-induced swelling at high suctions is primarily reversible (Fig. 4b).
- At lower values of suction (9 MPa for total stress of 0.1 MPa and 39 MPa for total stress of 5 MPa), the model is predicting heating-induced compaction (“collapse”). This compaction is irreversible and it is controlled by the offset of normal compression lines at different temperatures (by the parameters l_T and n_T). Still, for stress 0.1 MPa and suction 39 MPa the state is well within the state boundary surface and heating-induced swelling is predicted in agreement with experimental data.
- Upon cooling, the model is predicting cooling-induced contraction. This contraction depends on suction, such that it is most pronounced at high suction of 110 MPa and least significant at lower values of suction (39 MPa and 9 MPa). These predictions are governed by the dependency of the double-structure coupling factor f_m on macrostructural degree of saturation (Eq. (7)).

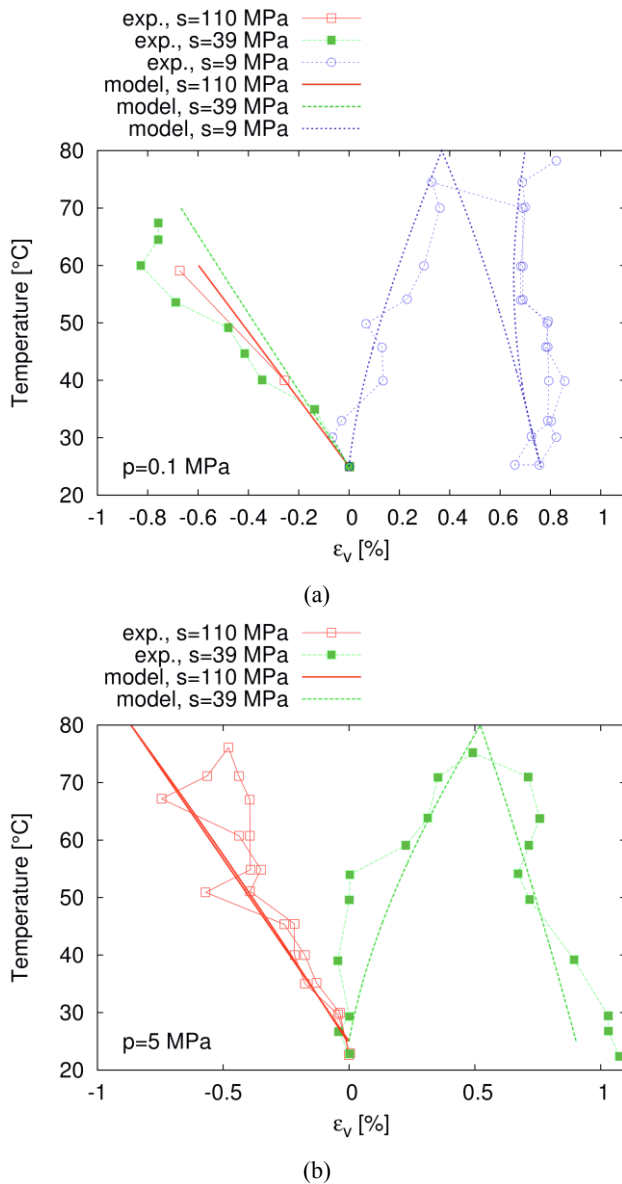


Figure 4. Volume change due to heating and cooling at total isotropic stresses of 0.1 MPa (a) and 5 MPa (b). Experimental data [11], compared with model predictions.

The isotropic compression at various values of suction and temperature is shown in Fig. 5. The model predicts reasonably the initial void ratio, implied by wetting-induced swelling during the preceding experimental stage. Considering the effect of temperature, the model predicts lower position of the isotropic normal compression lines at higher temperatures (the parameter n_t has a negative value). The difference appears to be insignificant in Fig. 5, but they are important to induce heating-induced compaction shown in Fig. 4.

Figure 5 shows that also the shape of the isotropic compression lines and the effect of suction on apparent preconsolidation pressure is predicted properly.

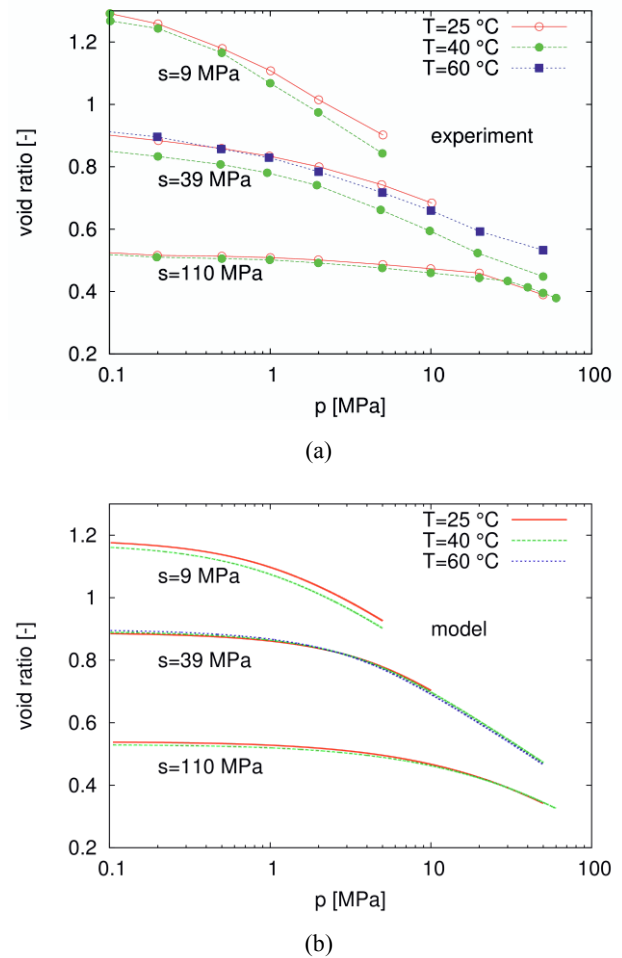


Figure 5. Isotropic compression tests at various suctions and temperatures. (a) experimental data from [11], (b) predictions.

4 Summary and conclusions

A new thermos-hydro-mechanical model for expansive soils based on double structure concept and hypoplasticity has been developed. In the paper, the most important properties of the model have been presented. It has been shown that the model provides correct predictions of the complex behaviour of MX80 bentonite under various thermo-hydro-mechanical paths.

In particular, the model properly predicts swelling or shrinkage in heating-cooling tests, depending on the current suction, total stress and void ratio. Also, global swelling of the samples due to wetting and the influence of suction and temperature on the shape of isotropic compression curves are well predicted. The model overpredicts the global water content at low values of suction, but this can potentially be caused by inconsistency in the two experimental data sets.

Acknowledgement

The author is grateful for the financial support by the research grant 15-05935S of the Czech Science Foundation.

References

1. E. E. Alonso, J. Vaunat, A. Gens, *Engineering Geology* **54**, 173-183 (1999)
2. S. Grant, A. Salehzadeh, *Water Resources Research* **32**, 261-270 (1996)
3. E. Romero, A. Gens, A. Lloret, *Geotechnical and Geological Engineering* **19**, 311-332 (2001)
4. D. Mašín, *Int. J. Numer. Anal. Meth. Geomech.* **34**, 73-90 (2010)
5. D. Mašín, *Acta Geotechnica* **8**, 481-49 (2013)
6. D. Mašín, *Engineering Geology* **165**, 73-88 (2013)
7. D. Mašín, N. Khalili, *Int. J. Numer. Anal. Meth. Geomech.* **32**, 1903-1926 (2008)
8. D. Mašín, N. Khalili, *Int. J. Numer. Anal. Meth. Geomech.* **36**, 17-35 (2012)
9. D. Mašín, N. Khalili, *Canadian Geotechnical Journal* (2015), doi: 10.1139/cgj-2014-0479
10. A. Tang, Y. Cui, *Canadian Geotechnical Journal* **42**, 287-296 (2007)
11. A. Tang, Y. Cui, *Géotechnique* **58**, 45-54 (2008)